Cerebral Cortex July 2009;19:1504-1514
doi:10.1093/cercor/bhn163
Advance Access publication October 1, 2008

Limbic Epileptogenesis in a Mouse Model of Fragile X Syndrome

Li-Feng Qiu[1], Ting-Jia Lu[1], Xiao-Ling Hu[1], Yong-Hong Yi[2], Wei-Ping Liao[2] and Zhi-Qi Xiong[1]

[1]Institute of Neuroscience and State Key Laboratory of Neuroscience, Shanghai Institutes for Biological Sciences, Chinese Academy of Sciences, Shanghai 200031, China and [2]Institute of Neuroscience and the Second Affiliated Hospital of Guangzhou Medical College, Guangzhou 510260, China

Fragile X syndrome (FXS), caused by silencing of the *Fmr1* gene, is the most common form of inherited mental retardation. Epilepsy is reported to occur in 20–25% of individuals with FXS. However, no overall increased excitability has been reported in *Fmr1* knockout (KO) mice, except for increased sensitivity to auditory stimulation. Here, we report that kindling increased the expressions of *Fmr1* mRNA and protein in the forebrain of wild-type (WT) mice. Kindling development was dramatically accelerated in *Fmr1* KO mice, and *Fmr1* KO mice also displayed prolonged electrographic seizures during kindling and more severe mossy fiber sprouting after kindling. The accelerated rate of kindling was partially repressed by inhibiting N-methyl-D-aspartic acid receptor (NMDAR) with MK-801 or mGluR5 receptor with 2-methyl-6-(phenylethynyl)-pyridine (MPEP). The rate of kindling development in WT was not effected by MPEP, however, suggesting that FMRP normally suppresses epileptogenic signaling downstream of metabolic glutamate receptors. Our findings reveal that FMRP plays a critical role in suppressing limbic epileptogenesis and predict that the enhanced susceptibility of patients with FXS to epilepsy is a direct consequence of the loss of an important homeostatic factor that mitigates vulnerability to excessive neuronal excitation.

Keywords: epilepsy, FMRP, kindling, mGluR5, mossy fiber sprouting, NMDA

Introduction

Fragile X syndrome (FXS), the most common form of inherited mental retardation, results from a trinucleotide repeat (CGG) expansion in the 5′-untranslated region of the gene *Fmr1* (Verkerk et al. 1991). The CGG repeat expansion and subsequent hypermethylation cause transcriptional silencing of *Fmr1* and loss of its encoded protein, the fragile X mental retardation protein (FMRP) (O'Donnell and Warren 2002; Jin and Warren 2003). Murine FMRP is a brain-specific RNA-binding protein that suppresses translation of target RNAs. Through interactions with kinesin, FMRP is able to travel between distal neurites and the soma of neurons and thereby regulate protein synthesis locally within specific cellular compartments (Ashley et al. 1993; Warren and Nelson 1994; Eberhart et al. 1996; Brown et al. 1998; Darnell et al. 2001; Li et al. 2001; Ohashi et al. 2002; Ling et al. 2004; Davidovic et al. 2007).

Patients with FXS exhibit mental retardation, attention deficits, autistic behavior, macroorchidism, and facial abnormalities (Turner et al. 1980; Opitz and Sutherland 1984; Sobesky et al. 1996). Additionally, epilepsy is reported to occur in 20–25% of individuals with FXS and paroxysmal electroencephalography (EEG) abnormalities are present in about 50% of prepubescent boys with FXS (Musumeci et al. 1999; Sabaratnam et al. 2001; Hagerman et al. 2002). These EEG pattern abnormalities resemble those of patients with benign focal epilepsy of childhood (Berry-Kravis 2002). FMRP deficiency is speculated to lead to increased neuronal excitability and susceptibility to seizures in humans. However, spontaneous seizures are never observed in *Fmr1* knockout (KO) mice and sensitivity to convulsants (such as bicuculline, pentylenetetrazol and kainic acid) is not significantly different from wild-type (WT) mice (Chen and Toth 2001). The most substantial deficit observed in *Fmr1* KO mice is increased sensitivity to auditory seizures (Musumeci et al. 2000; Chen and Toth 2001), suggesting that *Fmr1* KO mice do not have an overall increased excitability phenotype but rather auditory system specific hyperexcitability.

Recent studies have challenged this conclusion. In hippocampal slices from *Fmr1* KO mice, increasing neuronal activity by blocking γ-aminobutyric acidergic (GABAergic) transmission by the $GABA_A$ receptor antagonist bicuculline induces prolonged epileptiform discharges (Chuang et al. 2005). Furthermore, these prolonged discharges can be suppressed with the mGluR5 antagonist 2-methyl-6-(phenylethynyl)-pyridine (MPEP). These observations suggest that FMRP does influence neuronal excitability in the forebrain, possibly by repressing group I mGluR-mediated RNA translation (Chuang et al. 2005). Interestingly, MPEP could also reverse other symptoms of *Fmr1* KO mice, including sound-induced seizures (Bear et al. 2004; Chuang et al. 2005; McBride et al. 2005; Yan et al. 2005). These findings support the mGluR theory of FXS (Bear et al. 2004; Ronesi and Huber 2008).

To investigate seizure susceptibility in the limbic system of *Fmr1* KO mice in vivo, we used a well-established animal model of limbic epilepsy, amygdala kindling, to explore the role of FMRP in limbic epileptogenesis. Kindling mimics epileptogenesis in which repeated administration of an initially subconvulsive electrical stimulation of the amygdala results in progressive intensification of behavioral seizures and prolongation of electrographic afterdischarges (AD) (Goddard et al. 1969; Racine 1972). We found that kindling stimulation increased the expression of *Fmr1* mRNA and protein in the forebrain of WT mice. The development of behavioral seizures was dramatically accelerated in the *Fmr1* KO mice, and AD durations were greatly exaggerated throughout kindling. Furthermore, exuberant mossy fiber sprouting (MFS) was observed in fully kindled *Fmr1* KO mice. Behavioral seizures could be repressed by administering the N-methyl-D-aspartic acid receptor antagonist MK801 or mGluR5 antagonist MPEP in *Fmr1* KO mice. Interestingly, MPEP did not alter kindling development in WT mice, suggesting that FMRP normally suppresses the epileptogenic effects of mGluR5 activity. Our

findings indicate that FMRP-mediated transcriptional repression plays a critical role in moderating susceptibility to limbic epileptogenesis.

Materials and Methods

Experimental Animals

Male *Fmr1* KO mice of the FVB strain (The Dutch–Belgian Fragile X Consortium 1994) and their WT littermates were used. All animals were maintained on a 12:12 h light:dark cycle with a constant room temperature. Mice were group housed (3 to 4 per cage) and provided with ad lib food and water. Kindling experiments were conducted during the light phase of the cycle on 12-week-old adult mice. Mice were handled according to the guidelines prescribed by the Animal Care and Use Committee of the Institute of Neuroscience, Chinese Academy of Sciences. All efforts were made to minimize suffering and the number of animals used.

Drug Application

The NMDA antagonist MK801 (Sigma, St Louis, MO) and the mGluR5 antagonist MPEP (Tocris, Biotrend Chemikalien, Köln, Germany) were dissolved in sterile saline (0.9% NaCl). Drugs were administered by intraperitoneal injection (MK801, 0.5 mg/kg; MPEP, 30 mg/kg) 30 min before each stimulation. Application of the transcription inhibitor actinomycin D (Sigma) was performed on freely moving animals via a cannula inserted into ventricle (coordinates: 3 mm lateral and 2.3 mm posterior to bregma, 4 mm below dura) 30 min before a class 5 seizure-inducing stimulation. Actinomycin D was dissolved in saline (0.9% NaCl) to a final concentration of 50 μg/ul. Actinomycin D 5 μl was intracerebroventricular (i.c.v.) injected within 10 min.

Surgery and Kindling Procedure

A twisted bipolar electrode was implanted into the right amygdala (coordinates: 2.9 mm lateral and 1.2 mm posterior to bregma, 4.6 mm below dura) of animals under pentobarbital (60 mg/kg) anesthesia. Animals were then given 10 days to recover. The electrographic seizure threshold (EST) for each individual mouse was determined by applying 1-s train of 1-ms biphasic rectangular pulses at 60 Hz beginning at 50 μA. Additional stimulations increasing by 10 μA were administered at 2-min intervals until an electrographic seizure lasting at least 5 s was evoked. Stimulations at the EST intensity were subsequently applied once daily. EEGs and behavioral seizures were observed and recorded. The severity of the behavioral manifestations of seizures was classified according to the criteria of Racine (1972). Fully kindled is defined by the occurrence of 3 consecutive seizures of class 4 or greater. All surgery and kindling procedures were performed blind to genotype. Unstimulated control animals of each genotype underwent surgical implantation of an electrode in the amygdala and were handled identically but were not stimulated. Electrode placement was confirmed by methyl green pyronine-Y staining. Data derived from animals with correct electrode placement were analyzed.

RNA Extraction, cDNA Synthesis, Reverse Transcription Polymerase Chain Reaction, and Real-Time Polymerase Chain Reaction

Two weeks after being fully kindled, WT mice were killed either 3 h after a single class 5 seizure or without any further stimulation. Forebrains of unstimulated and stimulated fully kindled mice were dissected out and homogenized in a Trizol solution (100 mg of tissue/ml; Invitrogen, Carlsbad, CA). Samples were incubated for 5 min at room temperature before RNA extraction with chloroform for 3 min. After centrifugation at 12 000 × *g* for 15 min at 4 °C, the aqueous phase was transferred to a new tube, and total RNA was precipitated with isopropanol at –20 °C for a minimum of 1 h. RNA was washed in 75% ethanol, dissolved in nuclease-free water to a final concentration of 1 mg/ml, and stored at –80 °C.

First-strand cDNA was synthesized by priming 2 μg of total RNA with an oligo-dT primer and extending with M-MLV reverse transcriptase (Invitrogen) in a 20-μl reaction at 37 °C for 60 min. Products were then diluted into 100 μl. Four microliters of first-strand cDNA preparation were used as template in polymerase chain reaction (PCR) reactions with the following sense and antisense oligonucleotide primers: 1) P1 (5′-CTCAAAGCGAGCCCACAT) and P2 (5′-TACCATACCCTGCCAAGC), these primers direct the amplification of nucleotide 793 to 1456 of mouse *Fmr1* cDNA and 2) P3 (5′-CTGCCCAGAACATCATCCCT) and P4 (5′-CCACCACCCTGTTGC TGTAG), these primers direct the amplification of nucleotide 579 to 947 of mouse *Gapdh* cDNA. The cDNA was amplified with Taq polymerase under the following PCR conditions; for *Fmr1*: 28 cycles of denaturation at 94 °C for 30 s, annealing at 55 °C for 30 s, and extension at 72 °C for 1 min and for *Gapdh*: 20 cycles of 94 °C for 30 s, 60 °C for 30 s, and 72 °C for 1 min. PCR products were analyzed in 1% agarose gels.

Real-time PCR analysis of *Fmr1* expression was performed using SYBR Green I in a 20-μl reaction with an ABI Prism 7000 thermocycler (Applied Biosystems, Foster City, CA). Primers used for the amplification of *Fmr1* were P5 (5′-GTGGTTA GCTAAAGTGAGGATGAT) and P6 (5′-CAGGTTTGT-TGGGATTAACAGATC). Primers used to amplify *Gapdh* were the same as those listed above (P3 and P4). Products were amplified with HotStart ExTaqDNA polymerase under the following PCR conditions: denaturation at 95 °C for 5 min followed by 45 cycles of 10 s at 95 °C and 31 s at 60 °C. Dissociation curve analysis was performed after amplification to confirm the absence of nonspecific amplification products and primer–dimers. Real-time PCR results were analyzed with ABI Prism SDS 7000 software (Applied Biosystems).

In Situ Hybridization

Two weeks after being fully kindled, WT mice were perfused transcardially for 10 min with 4% paraformaldehyde in 0.1 M phosphate buffer (PB, pH 7.4) either 3 h after a single class 5 seizure or without any further stimulation. Brains were removed and postfixed in the same fixative for 4 h at 4 °C. After postfixation, brains were immersed in 20% sucrose in PB overnight at 4 °C. Coronal cryostat sections (20 μm) were mounted onto Fisher Super Frost Microscope slides and stored at –80 °C.

Antisense probes against *Fmr1* nucleotides 1126–1670 were designed. Reverse transcription polymerase chain reaction (RT-PCR) products were subcloned into pEGM-T-Easy vector (Promega, Madison, WI) and digoxigenin (DIG)-labeled sense and antisense ribonucleotide probes were generated by in vitro transcription using T7 and Sp6 RNA polymerases. Slides were prehybridized in hybridization buffer for 4 h at 65 °C and then hybridized with probes (1 μg/ml) in hybridization buffer at 65 °C overnight. After extensive washing, slides were incubated with preabsorbed alkaline phosphatase–conjugated anti-DIG antibody (Roche, Switzerland) at 4 °C overnight. Signals were developed by nitrotetrazolium blue-5-bromo-4-chloro-3-indolyl phosphate color reaction in the dark for 6–8 h. Samples were analyzed under a Nikon E600FN upright microscope.

Western Blot

Frozen forebrains extracted at the time points described in the Results section were thawed on ice and homogenized in lyses buffer containing 50 mM Tris-HCl (pH 7.4), 20 μg/ml leupeptin, 20 μg/ml aprotinin, 0.1 mM phenylmethylsulfonyl fluoride, 1 mM EDTA, 1 mM sodium orthovanadate, 1.0% deoxycholate. The homogenate was incubated on ice for 30 min to allow complete lyses and then centrifuged for 20 min at 14 000 × *g* (4 °C) to remove nuclear fractions, and protein concentrations were then determined using the bicinchoninic acid kit (BCA kit; Pierce, Rockford, IL). Proteins were separated by 9% sodium dodecyl sulfate–polyacrylamide gel and transferred to nitrocellulose membranes with a transblot semi-dry apparatus (Bio-Rad, Hercules, CA). Membranes were blocked in Tris-Buffered Saline Tween-20 (TBST; 0.05% Tween-20 in TBS) containing 5% dehydrated fat-free milk for 1 h and then incubated with anti-FMRP monoclonal antibody 1C3 (1:500; Chemicon, Temecula, CA) or anti-Glyceraldehyde 3-phosphate dehydrogenase monoclonal antibody (1:5000, KangChen, Shanghai, China) at 4 °C overnight. Membranes were washed in TBST buffer and incubated for 1 h with horseradish peroxidase–conjugated goat anti-mouse secondary antibody (1:5000, Chemicon) at room temperature. Immunoblots were developed with enhanced chemiluminescence (Pierce). Quantitative

analysis was conducted using Image Quant software (Molecular Dynamics, Sunnyvale, CA).

Immunohistochemistry

Free-floating sections were treated in 1% H_2O_2 for 30 min at room temperature and incubated for 5 min in 0.5% Triton X-100, washed in phosphate-buffered saline (PBS), and blocked with 5% NGS in PBS for 1 h at room temperature. Slices were then incubated with anti-FMRP (1:200; Chemicon) overnight at 4 °C, washed, and incubated with biotinylated goat anti-mouse IgG (1:200; Boster, Wuhan, China) for 1 h at room temperature. After being washed with PBS, slices were reacted with peroxidase-conjugated avidin–biotin complexes (Vector, Burlingame, CA; 1 h) for 1 h at room temperature. Signals were developed with 0.03% 3,3-diaminobenzidine tetrahydrochloride dihydrate (Sigma) in 50 mM Tris buffer containing 0.003% H_2O_2, pH 7.6. Negative control sections were prepared by omitting primary antibodies. Samples were analyzed under a Nikon E600FN upright microscope.

The Fluoro-Jade B Staining

For cell death analyses, both kindled WT and *Fmr1* KO mice were sacrificed 24 h after being fully kindled. WT and *Fmr1* KO brain sections were prepared as described in the In Situ Hybridization. Mounted sections were rehydrated in an ethanol series (3 min 100% ethanol, 1 min 70% ethanol, 1 min 50% ethanol, and 1 min distilled water) and then incubated in a solution of 0.06% potassium permanganate for 10 min on a rotating platform, rinsed in distilled water for 2 min, and transferred to fluoro-jade B (FJB) staining solution (0.0004% FJB in 0.1% acetic acid, prepared 10 min before use) for 20 min. Labeled sections were imaged with a confocal laser-scanning microscope (Olympus LSM-GB200) under green (FJB) fluorescence. Staining and data analysis were done by an individual blinded to the genotype and treatment.

Timm Staining

Fully kindled WT and *Fmr1* KO mice were killed either 5 or 28 weeks later after the last stimulation. Mice were perfused transcardially with saline for 2 min, followed by 0.16% sodium sulfide in PB for 4 min, and followed by saline for 1 min and 4% paraformaldehyde in PB for 10 min. Brains were then removed and postfixed overnight at 4 °C and immersed in 20% sucrose at 4 °C the following night. Horizontal sections (20 μm) were collected in PBS (pH 7.4) and mounted onto gelatin-coated slides and developed in the dark at room temperature for 30–50 min in a 12:6:2:1 mixture of gum arabic (50% w/v), hydroquinone solution (5.67% w/v), citric acid–sodium citrate buffer (26% citric acid w/v; 24% sodium citrate, w/v), and silver nitrate (17% w/v). After washing thoroughly with running water, sections were dehydrated, cleared in xylene, and coverslipped.

To assess MFS, the Timm index was measured using Image-Pro Plus 5.0 software (Media Cybernetics, Bethesda, MD) by dividing the total area of Timm granules by total length of dentate gyrus (DG; Watanabe et al. 1996). The Timm index of each mouse was calculated as the mean value of 3 serial sections through the hippocampus of each animal.

Nissl Staining and Cell Number Counting

Cell death was assessed in serial horizontal sections (20 μm) through the hippocampus. Every third slice between 4000 and 5300 μm ventral from the dorsal surface of neocortex were placed into 1:1 alcohol:chloroform for 30 min and then rehydrated in an ethanol series (3 min each in 100%, 95%, 80%, 70%, 60%, 50%, and 0% ethanol in distilled water). Rehydrated slices were stained in cresyl violet solution for 30 min at room temperature then dehydrated (3 min each in 50%, 60%, 70%, 80%, 95%, and 100% ethanol), cleared in xylene and mounted with resinous medium, and analyzed under a Nikon E600FN upright microscope. Cells in the hilus field were counted using Image-Pro Plus 5.0 software (Media Cybernetics).

Statistical Analysis

Statistical analyses were carried out with GraphPad Prism Software (San Diego, CA). For statistical analyses of kindling development, Timm indices, and cell number, analyzers were blinded to the genotypes and treatment. Kindling development data and real-time PCR result were compared with unpaired *t*-test analysis, Timm indices were compared with 2-way ANOVA, post hoc Bonferroni's test. Cell number and western blots were compared with 1-way ANOVA, post hoc Dunnett's test.

Results

The Expressions of Fmr1 mRNA and FMRP are Upregulated by Seizure Activity

Previous studies have demonstrated that the expression of FMRP can be regulated by synaptic activity and experience (Weiler et al. 1997; Todd and Mack 2000; Todd et al. 2003; Gabel et al. 2004; Hou et al. 2006). To examine whether seizure activity regulates *Fmr1* transcription, we investigated the level of *Fmr1* mRNA expression after kindling-induced seizures (see Materials and Methods for a description of kindling procedures) by RT-PCR, real-time PCR, and in situ hybridization. Two weeks after being fully kindled, WT mice were killed either 3 h after a single stimulation, which was given to trigger a class 5 seizure, or without any further stimulation. RT-PCR and real-time PCR were performed using RNA from the forebrain of both unstimulated kindled WT mice and stimulated kindled WT mice. As shown in Figure 1*A*, the level of *Fmr1* mRNA in the forebrain normalized to *Gapdh* increased significantly 3 h after kindling-induced seizure. Real-time PCR analysis showed that a single class 5 seizure caused a 2-fold increase of *Fmr1* mRNA ($n = 8$) relative to unstimulated kindled mice ($n = 8$, $P < 0.05$). In situ hybridization revealed that *Fmr1* expression was strongly induced in the cortex from low baseline levels 3 h after seizure activity. *Fmr1* expression was also upregulated in the hippocampal CA1 region and DG, albeit to a lesser degree and from a higher baseline (Fig. 1*B*). All changes in *Fmr1* mRNA expression after kindling stimulations were bilateral with no hemispheric bias. No difference in *Fmr1* mRNA expression was observed between unstimulated fully kindled WT mice and unkindled, sham-stimulated controls (data not shown).

We next examined if the upregulation of *Fmr1* mRNA by seizure activity resulted in a corresponding increase in protein expression. Total protein lysates from individual forebrains were assayed by western blot. The mean level of FMRP normalized to Gapdh in the forebrain of unstimulated fully kindled mice was essentially identical to that of unkindled controls (data not shown). As shown in Figure 2*A*, FMRP expression increased about 5-fold 3 h after class 5 seizure activity in kindled mice ($n = 8$) relative to unstimulated fully kindled mice ($n = 12$, $P < 0.01$), before declined back to baseline levels by 12 h (Fig. 2*B*).

To investigate the spatial distribution of seizure-induced FMRP expression, we performed immunohistochemical staining on hippocampal sections. In unstimulated fully kindled mice, FMRP was primarily expressed in the soma of CA1 pyramidal neurons and DG granule cells, similar to unkindled controls (Fig. 2*C* and data not shown). However, 3 h after a single class 5 seizure, the intensity of FMRP immunostaining was greatly increased in the soma of CA1 pyramidal neurons and in the soma of DG granule cells (Fig. 2*C*, right panel). No obvious immunostaining of either the dendrites or the nucleus of neurons in the hippocampus was observed in control or stimulated animals.

To investigate whether the expression of FMRP correlates with the development of kindling, we examined the expression of FMRP at different stages during kindling development. Protein lysates from the forebrain were extracted 3 h after the

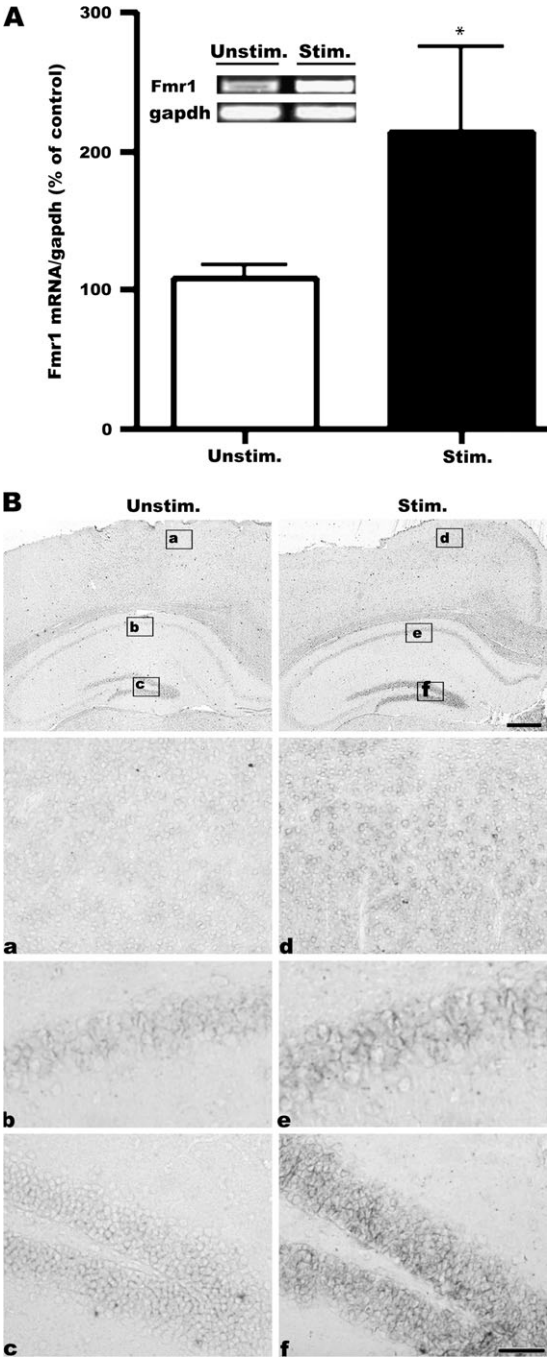

Figure 1. Kindling upregulates *Fmr1* mRNA in the forebrain. (*A*) Quantitative real-time PCR (lower) and RT-PCR (upper) analysis of *Fmr1* mRNA expression. Total RNA was isolated from forebrains of fully kindled WT mice 3 h after an evoked class 5 seizure (Stim.) or without any further stimulation (Unstim.). *Fmr1* mRNA was normalized to G*apdh* mRNA levels and mean ± standard error of the mean values are presented as a percentage of unstimulated controls; $^{*}P < 0.05$, unpaired *t*-test. (*B*) *Fmr1* in situ hybridization of coronal sections from unstimulated fully kindled WT mice (left panel) and fully kindled WT mice 3 h after seizure (right panel). In the unstimulated group, *Fmr1* expression is relatively low in the cortex (a), the CA1 and the DG (b and c). Three hours after a class 5 seizure, *Fmr1* mRNA is upregulated in both the cortex (d) and hippocampus (e and f). Lower panels show higher magnification images of the areas indicated by the boxes in the upper panels. Scale bars: upper panel, 400 μm in upper panel; lower panel, 50 μm.

first stimulation on the first day of kindling (1 stimulation; AD duration, 8.1 ± 0.5 s), 3 h after the first class 2 seizure (5 ± 1 stimulations; AD duration of class 2 seizure, 19.2 ± 2.7 s), or 3 h after the third consecutive class 4/5 seizure (12 ± 1 stimulations; AD duration of final class 4/5 seizure, 26.9 ± 2.2 s). Relative to sham-stimulated controls, no increase in FMRP was observed 3 h after the initial subconvulsive stimulation (data not shown), but FMRP expression in the forebrain significantly increased after the first class 2 seizure and was further enhanced after full kindling (Fig. 2*D*). Statistical analysis showed about a 3.5-fold increase of FMRP expression after class 2 seizure ($n = 5$) and 5.2-fold increase of FMRP expression in fully kindled mice ($n = 8$) compared with controls ($n = 17$; $P < 0.05$ and $P < 0.001$, respectively) (Fig. 2*E*). Taken together, these data reveal that both mRNA and protein expression of *Fmr1* gene are upregulated by kindling-induced seizure activity in vivo.

Finally, in order to decipher the transcriptional versus translational mechanisms of the seizure-induced upregulation of FMRP, we i.c.v. injected the transcription inhibitor actinomycin D 30 min before a class 5 seizure-inducing stimulation and then assayed *Fmr1* mRNA or protein levels in the forebrain 3 h after by RT-PCR or western blotting. Actinomycin D did block the seizure-induced increase in the level of *Fmr1* mRNA ($n = 3$; $P < 0.05$; Fig. 2*F*), but the increase in protein level was unaffected (Fig. 2*G*). This data suggests that seizure activity-induced upregulation of FMRP protein in WT mice is largely due to changes in the rate of translation.

Accelerated Development of Kindling in Fmr1 KO Mice

To study the functional significance of seizure-regulated FMRP expression, seizure behaviors and AD durations of WT and *Fmr1* KO mice after daily amygdala stimulations were compared. There was no significant difference in EST between the 2 groups (Fig. 3*A*). The mean EST for WT and *Fmr1* KO mice were 141.4 ± 9.77 μA ($n = 25$) and 139.7 ± 10.71 μA ($n = 31$), respectively. Once-daily stimulation of the amygdala resulted in progressive increase in the intensity of behavioral seizures in *Fmr1* KO mice as in WT mice. However, the rate at which behavioral seizures progressed was dramatically accelerated in *Fmr1* KO mice (Fig. 3*B*) with the number of stimulations required to induce 3 consecutive class 4/5 seizures (5.45 ± 0.40, $n = 25$) reduced to about half of the number of stimulations required for WT mice (11.5 4 ± 0.45, $n = 31$, $P < 0.001$) (Fig. 3*C*).

The differences in behavioral seizure intensity were paralleled by differences in electrophysiological measures of seizure duration. F*mr1* KO mice displayed prolonged AD after repeated kindling stimulations (Fig. 4). By the third day of stimulation, the AD duration was doubled compared with that of WT mice (Fig. 4*A*). In WT mice, the duration of AD reached about 30 s by the 14th stimulation and additional stimulation did not induce any further prolongation of AD duration. In sharp contrast, the AD duration reached 30 s after only 3 stimulations in *Fmr1* KO mice and climbed up to over 45 s by the 14th stimulation (Fig. 4*A*). Representative electrographs are shown in Figure 4*B*.

Effects of NMDA Receptor and mGluR5 Antagonists on Epileptogenesis

Studies of several animal models have shown that activation of ionotropic (Croucher et al. 1995) and metabotropic glutamate receptors (Wong et al. 1999) can promote epileptogenesis. We speculated that FMRP might function to suppress seizure-promoting actions of either one or both classes of glutamate receptors. To test this, we treated *Fmr1* KO mice with the

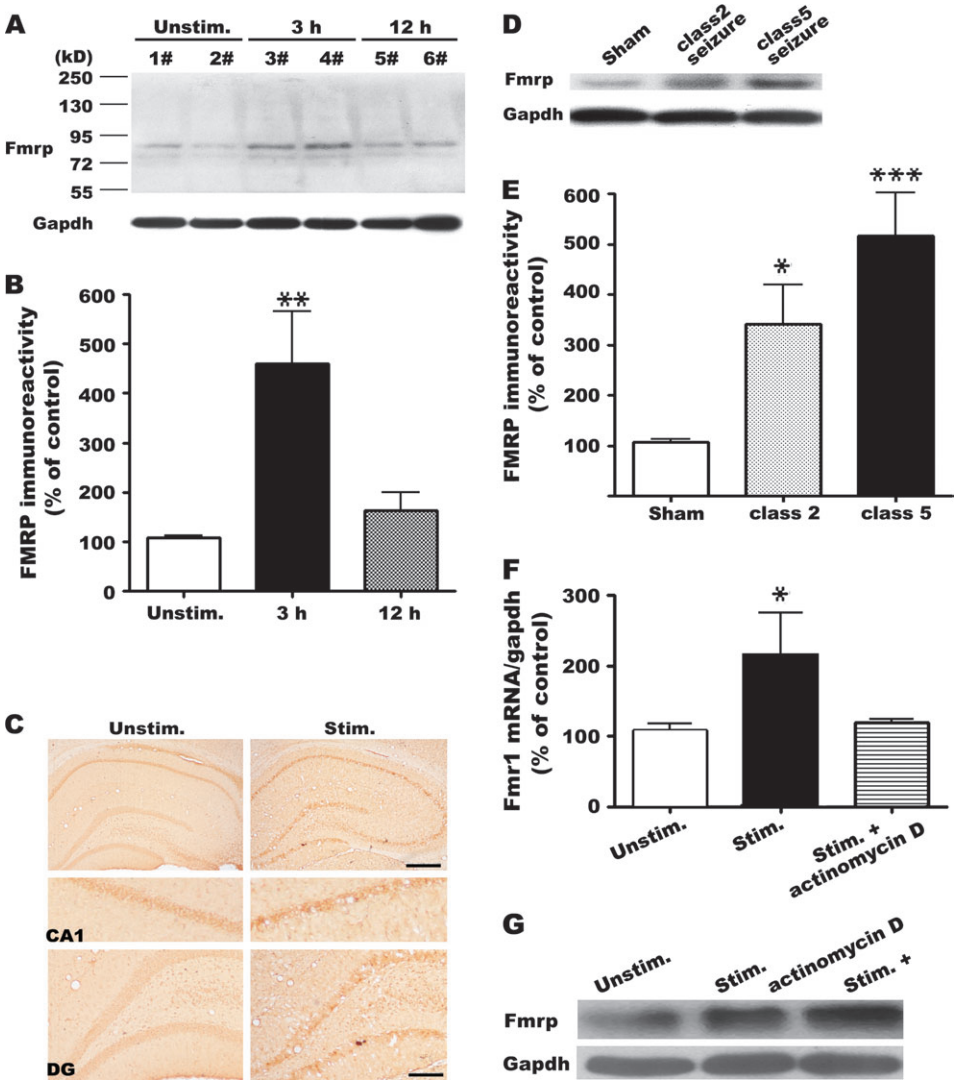

Figure 2. FMRP expression is upregulated after seizure activity. (*A*) Representative western blot showing a transient increase of FMRP in the forebrain of kindled mice after an evoked seizure. Two weeks after fully kindling, a single class 5 seizure was induced in WT mice and forebrains were isolated 3 h or 12 h later. Each lane was loaded with an equal amount of protein extract from a single forebrain sample (mouse #1–6). Lane 1 and 2, unstimulated fully kindled WT mice; lane 3 and 4, fully kindled mice 3 h after a class 5 seizure; lane 5 and 6, fully kindled mice 12 h after a class 5 seizure. After a class 5 seizure, FMRP expression increases before returning to baseline levels by 12 h. (*B*) Quantitative analysis of western blot band intensities. FMRP immunoreactivity was normalized to Gapdh immunoreactivity and mean ± standard error of the mean (SEM) values are presented as a percentage of the mean level in unstimulated fully kindled mice; $^{*}P < 0.05$; $^{**}P < 0.01$; $^{***}P < 0.001$; 1-way ANOVA followed by post hoc Dunnett's test. (*C*) Seizure activity leads to increased FMRP expression in the soma of CA1 pyramidal cells and granule cells in the DG. Coronal sections through the hippocampus of unstimulated fully kindled WT mice (left panel) and fully kindled WT mice 3 h after a class 5 seizure-inducing stimulation (right panel) were immunolabeled with anti-FMRP. Lower panels show higher magnification of upper panel, note that no staining is observed in neurites and nucleus of hippocampal neurons. Scale bars: 400 μm for upper 1 row; 100 μm for lower 2 rows. (*D*) Upregulation of FMRP correlates with kindling development. Forebrains of WT mice isolated 3 h after sham stimulation (lane 1), 3 h after the first class 2 seizure during kindling (lane 2), or 3 h after the third class 5 seizure during kindling (lane 3). (*E*) Quantitative analysis of FMRP expression in (*D*). FMRP levels were normalized to Gapdh and mean ± SEM values are presented as a percentage of the mean level in sham-stimulated mice; $^{*}P < 0.05$; $^{**}P < 0.01$; $^{***}P < 0.001$; 1-way ANOVA with post hoc Dunnett's test. (*F*) Real-time PCR of *Fmr1* RNA from control mice, saline-treated stimulated mice, actinomycin D-treated stimulated mice. *Fmr1* transcript levels were upregulated at 3 h after stimulation in saline-treated mice and application of actinomycin D 30 min before stimulation repressed the increase of *Fmr1*. *Gapdh* transcript levels were used to normalize the levels of *Fmr1* and values are presented as group mean ± SEM as a percentage of unstimulated samples; $^{*}P < 0.05$; 1-way ANOVA, post hoc Dunnett's test. (*G*) Representative western blot showing that application of actinomycin D did not obviously repress seizure-induced increases of FMRP.

noncompetitive NMDA receptor open-channel blocker MK801 or the metabolic glutamate receptor mGluR5 antagonist MPEP. Consistent with previous studies (McNamara et al. 1988; Sato et al. 1988; Löscher and Hönack 1991), the rate of kindling in WT mice was slowed down during the first 2 weeks of stimulation when MK801 was injected 30 min before each daily stimulation relative to controls injected with saline (Fig. 5*A*). Interestingly, for the first 9 days of stimulation, the acceleration of kindling development in *Fmr1* KO mice was also suppressed by MK801 (Fig. 5*B*). During this period, there was no significant difference in the average seizure class between MK801 treated WT mice (n = 13) and MK801 treated *Fmr1* KO mice (n = 13). After the 10th stimulation, kindling development in MK801-treated *Fmr1* KO mice dramatically accelerated compared with the MK801-treated WT mice. These observations implicate the involvement of NMDARs in the progression of kindling in both WT and *Fmr1* KO mice, and FMRP ablation does not obviously alter the suppressive effect of inhibiting NMDAR on kindling development.

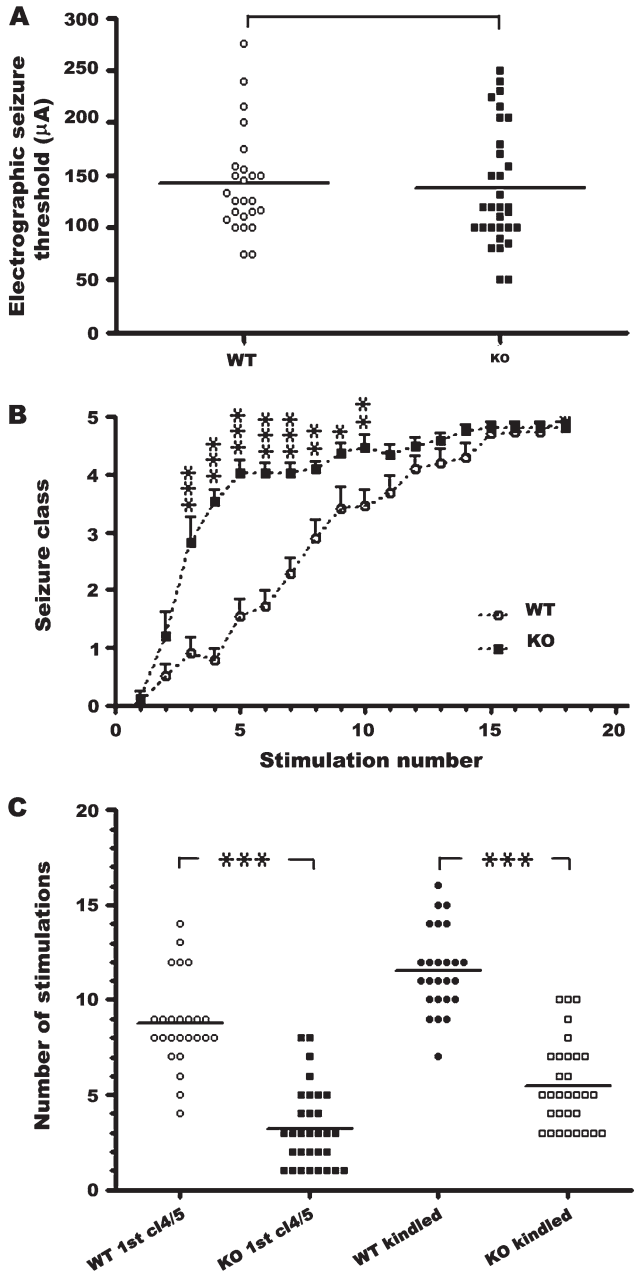

Figure 3. Striking acceleration of kindling development in *Fmr1* KO mice. (*A*) No significant difference between WT and *Fmr1* KO in mean EST is observed; $P = 0.77$, unpaired *t*-test. (*B*) Behavioral seizure intensities (class 1–5) evoked by amygdala stimulation at the predetermined EST, presented as mean ± SEM of WT mice ($n = 25$) and *Fmr1* KO mice ($n = 31$). (*C*) Number of stimulations required to provoke the first episode of class 4/5 seizure and third consecutive episode of class 4/5 seizure in WT mice ($n = 25$) and *Fmr1* KO mice ($n = 31$) mice; $^{***}P < 0.001$; 2-tailed unpaired *t*-test.

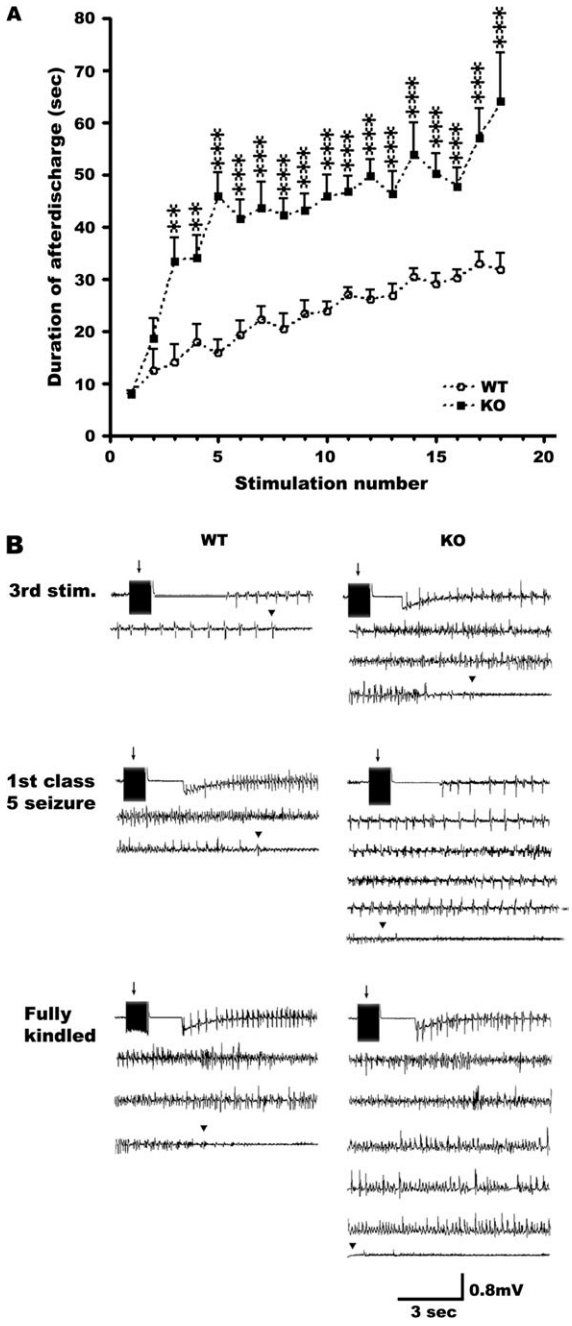

Figure 4. *Fmr1* KO mice exhibit prolonged electrographic seizures. (*A*) AD durations evoked by amygdala stimulation at the predetermined EST. The progressive prolongation of AD durations was significantly accelerated in *Fmr1* KO mice compared with WT mice. Data presented as mean ± standard error of the mean of WT mice ($n = 25$) and *Fmr1* KO mice ($n = 31$). (*B*) Representative EEG recordings of WT and *Fmr1* KO mice at the third stimulation, first class 5 seizure-inducing stimulation and third consecutive class 5 seizure-inducing stimulation. Arrows indicate the application of stimulation, and the arrowheads indicate the termination point of the electrographic seizure.

In WT animals, pretreatment with MPEP (30 mg/kg) 30 min before each daily stimulation did not significantly affect the development of kindling (Fig. 6*A*), consistent with previous study (Nagaraja et al. 2004). There was no significant difference in the average seizure class between the saline-treated WT mice ($n = 25$) and MPEP-treated WT mice ($n = 15$) at any time point throughout kindling (Fig. 6*A*). In contrast, application of MPEP significantly decelerated the rate of kindling progression in *Fmr1* KO mice up to the ninth day of stimulation. The average seizure class from the fourth through to the eighth stimulation point in MPEP-treated *Fmr1* KO mice ($n = 13$) was significantly lower than saline-treated *Fmr1* KO mice ($n = 31$) (Fig. 6*B*). Together, this data suggests that FMRP normally suppresses epileptogenic mGluR5 signal transduction and this activity is disinhibited in *Fmr1* KO mice, thus accelerating kindling development.

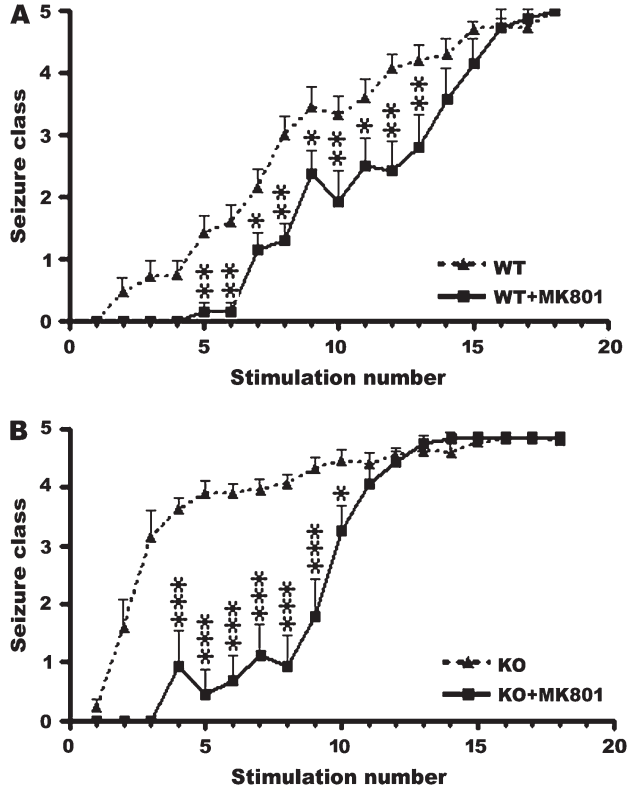

Figure 5. Effects of the NMDA antagonist MK801 on kindling development in WT and *Fmr1* KO mice. (*A*) Behavioral seizure intensities evoked by amygdala stimulation at the predetermined EST, data presented as mean ± standard error of the mean (SEM) of saline-treated WT ($n = 25$) and MK801-treated WT mice ($n = 13$). (*B*) Behavioral seizure intensities evoked by amygdala stimulation at the predetermined EST, data presented as mean ± SEM of saline-treated ($n = 31$) and MK801-treated *Fmr1* KO mice ($n = 13$). MK801 significantly slowed kindling development in both WT mice and *Fmr1* KO mice. Saline or MK801 was administered 30 min before each stimulation. Asterisks indicate statistically significant differences in the average behavior seizure class at the indicated time point between the 2 presented groups. $^{*}P < 0.05$; $^{**}P < 0.01$; $^{***}P < 0.001$; 2-tailed unpaired *t*-test.

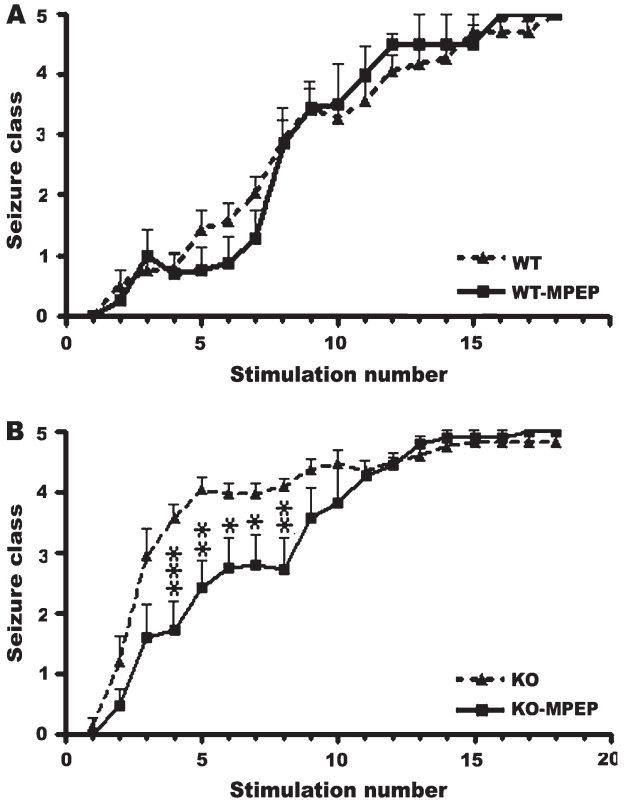

Figure 6. Effects of the mGluR5 antagonist MPEP on kindling development in WT and *Fmr1* KO mice. (*A*) Behavioral seizure class evoked by amygdala stimulation at the predetermined EST, data presented as mean ± standard error of the mean (SEM) of saline-treated ($n = 25$) and MPEP-treated WT mice ($n = 15$). There is no significant difference between kindling development in WT mice treated with MPEP compared with controls. (*B*) Behavioral seizure class evoked by amygdala stimulation at the predetermined EST, data presented as mean ± SEM of saline-treated ($n = 31$) and MPEP-treated *Fmr1* KO mice treated ($n = 13$). Administering MPEP to *Fmr1* KO mice significantly represses seizure intensities at the fourth through eighth stimulation point. Saline or MK801 was administered 30 min before each stimulation. Asterisks indicate statistically significant differences in the average behavior seizure class at the indicated time point between the 2 presented groups. $^{*}P < 0.05$; $^{**}P < 0.01$; $^{***}P < 0.001$; 2-tailed unpaired *t*-test.

Enhancement of Mossy Fiber Sprouting in Fully Kindled fmr1 KO Mice

MFS, characterized by an abnormal projection of the axon collaterals of granule cells into the inner molecular layer (IML) of the DG of the hippocampus (Sutula et al. 1989), is a feature of neuronal circuit reorganization associated with limbic epilepsy. We examined axon projections of hippocampal granule cells by Timm staining of WT and *Fmr1* KO mice, 5 weeks or 28 weeks after 22 consecutive days of stimulation. Representative Timm-stained hippocampal sections from both kindled and age-matched, sham-stimulated WT and *Fmr1* KO mice are shown in Figure 7A. The innervation's pattern in sham-stimulated *Fmr1* KO mice ($n = 13$) was not obviously different from that in sham-stimulated WT mice ($n = 8$) (Fig. 7*A*, d vs. a and j vs. g; Fig. 7*B*). Interestingly, striking enhancement of MFS in the IML was observed 5 weeks after 22 daily stimulations in the fully kindled *Fmr1* KO mice, but no change was observed in fully kindled WT mice (Fig. 7*A*, e vs. b, k vs. h; Fig. 7*B*). Twenty-eight weeks after 22 daily stimulations, a slight increase of Timm staining in the IML was detected in WT kindled mice (Fig. 7*A*, i vs. g; Fig. 7*B*) but was less severe than that in *Fmr1* KO mice 5 weeks after stimulation. At the 28 week time point, MFS in fully kindled *Fmr1* KO mice was further enhanced (Fig. 7*A*, l vs. k). Statistical analyses revealed a 10-fold increase of Timm index in the IML of the DG in the 5 weeks later killed fully kindled *Fmr1* KO mice and a 40-fold increase in 28 weeks later killed fully kindled *Fmr1* KO mice compared with their age-matched fully kindled WT mice (Fig. 7*B*). The enhancement of Timm staining after kindling in *Fmr1* KO mice was selective to the IML region. To determine whether the enhanced MFS in *Fmr1* KO mice was accompanied with an increase in neuronal cell loss, we performed Fluoro-Jade B staining and Nissl staining (Fig. 8) of brain sections from kindled mice. No obvious neuronal degeneration was detected in either fully kindled WT or *Fmr1* KO mice.

Discussion

Four principal findings emerged from this study. First, kindling induced by repeated electrical stimulations of the amygdala resulted in upregulation of the *Fmr1* gene in the forebrain. Second, the development of kindling, as measured by behavioral and electrophysiological indices, was accelerated in *Fmr1* KO mice. Third, inhibiting NMDAR slowed the early

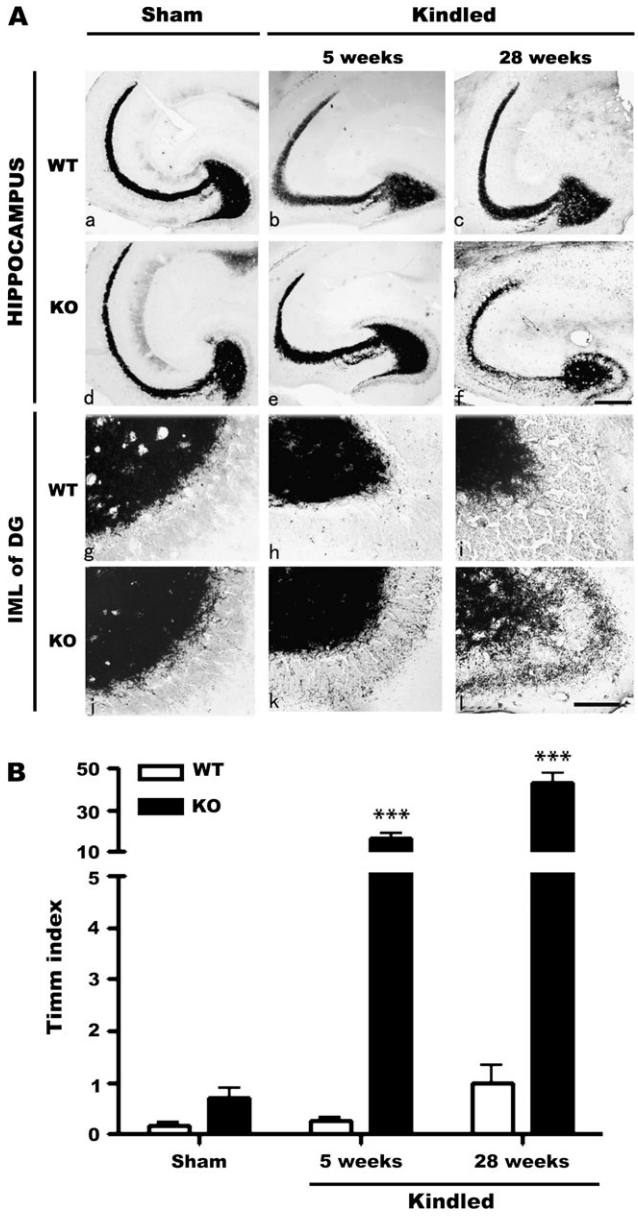

Figure 7. Axon projections of granule cells in the hippocampus of sham-stimulated and fully kindled WT and *Fmr1* KO mice. (*A*) Representative Timm staining of horizontal brain sections of sham-stimulated (sham) WT mice (a, g); sham *Fmr1* KO mice (d, j); fully kindled (kindled) WT mice 5 weeks (b, h) or 28 weeks (c, i) after 22 daily stimulation; kindled *Fmr1* KO mice 5 weeks (e, k) or 28 weeks (f, l) after 22 daily stimulations. Under control conditions (sham), *Fmr1* KO mice show slightly more Timm-stained granules in the granule cell body layer compared with WT mice. Five weeks after 22 daily stimulations, MFS is obvious in the IML of the DG in *Fmr1* KO mice. Twenty-eight weeks after 22 daily stimulations, MFS is dramatically more severe in *Fmr1* KO mice. In contrast, WT mice show little MFS 28 weeks after 22 daily stimulations. Scale bars: upper 2 panels, 250 μm; lower 2 panels, 50 μm. (*B*) Statistical analysis of Timm index in the IML of the DG. Bars represent mean ± standard error of the mean. ***$P < 0.001$; 2-way ANOVA with post hoc Bonferroni's test.

progression of kindling development in both WT and *Fmr1* KO mice. By contrast, inhibiting mGluR5 partially repressed the development of kindling in *Fmr1* KO mice but had little effect on kindling development in WT mice. Forth, kindling-induced MFS into the IML region of the DG was dramatically enhanced in *Fmr1* KO mice.

FMRP is upregulated in response to neuronal activity (Weiler et al. 1997; Todd and Mack 2000; Todd et al. 2003;

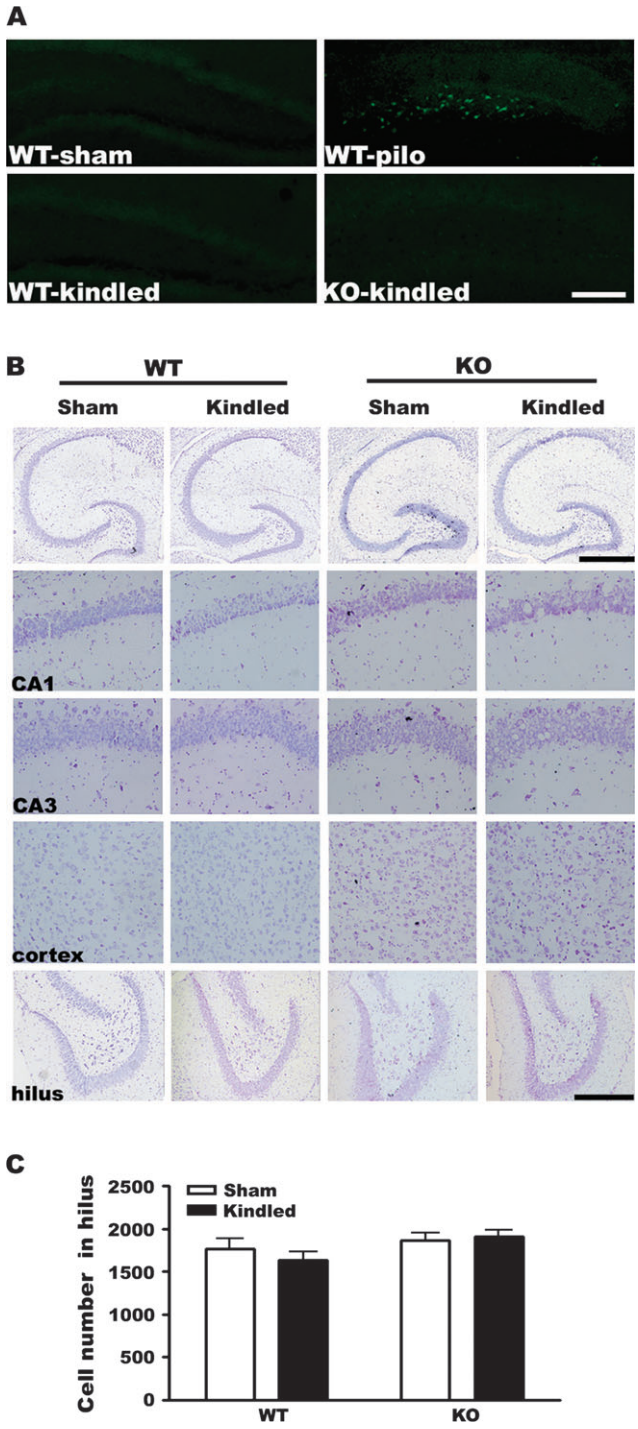

Figure 8. Fluoro-Jade B and Nissl staining reveal no obvious neuronal cell loss in *Fmr1* KO mice after kindling. (*A*) Fluoro-Jade B staining. A WT hippocampal section 24 h after pilocarpine-induced seizure (340 mg/kg, intraperitoneally) with significant cell death in the hilus of the DG is shown as a positive control ($n = 3$). No cell death is detected in sections from sham WT ($n = 3$), kindled WT ($n = 6$), or kindled *Fmr1* KO ($n = 6$) mice 24 h after the third consecutive class 5 seizure. Scale bar: 400 μm. (*B*) Nissl staining. Nissl-stained brain sections from sham WT mice, kindled WT mice, sham *Fmr1* KO mice, and kindled *Fmr1* KO mice reveal similar cell densities in the CA1, CA3, cortex, and hilus of the DG. Scale bars: top, 500 μm for upper one row; bottom, 250 μm for other rows. (*C*) Statistical analysis of cell number in the hilus. No significant difference was found among the 4 groups. Bars represent mean ± standard error of the mean; 1-way ANOVA, post hoc Dunnett's test.

Gabel et al. 2004; Irwin et al. 2005; Hou et al. 2006) and plays an important role in synaptic plasticity by regulating the translation, subcellular localization, and stability of specific mRNA targets (Brown et al. 2001; Darnell et al. 2001; Zhang et al. 2001; Miyashiro et al. 2003; Zalfa et al. 2003; Antar et al. 2004). Although FMRP can be translocated to distal compartments of neurons and regulate local translation of target mRNA, we observed increased FMRP immunoreactivity only in the cell body of CA1 and DG cells after seizure activity and did not detect FMRP within the neurites or nucleus of these cells.

Several findings have pointed a role for both ionotropic (Croucher et al. 1995) and metabotropic (Wong et al. 1999) glutamate receptors in promoting seizure activity in various animal models of epilepsy. To test the involvement of glutamate receptors in the expedited development of kindling, we treated *Fmr1* KO mice with the NMDA receptor antagonist MK801 or the mGluR5 antagonist MPEP. The loss of *Fmr1* did not obviously influence the dynamics of kindling development under conditions of NMDA receptor inhibition. However, blocking mGluR5 dramatically slowed the rate of kindling development exclusively in *Fmr1* KO mice. This suggests that enhanced seizure susceptibility in the *Fmr1* KO mouse is at least partially mediated by abnormal activation of mGluR5-dependent signal transduction which is largely suppressed in WT mice. This is consistent with the former finding that Group I mGluR and FMRP function in a convergent way in regulating mRNA translation and subsequently regulate synaptic plasticity and neuronal excitability (Greenough et al. 2001; Bear et al. 2004; Chuang et al. 2005; Hou et al. 2006; Nosyreva and Huber 2006; Pan and Broadie 2007; Pan et al. 2008).

The development of kindling in *Fmr1* KO mice have 3 interesting characteristics: normal EST, accelerated development of kindling, and prolonged electrographic seizures. These features share strong similarity to those observed in α2A adrenergic receptor (α2A-AR) null mice in which the number of stimulations required to achieve full kindling is reduced by about half and the duration of AD is nearly doubled throughout the development of kindling compared with WT mice (Janumpalli et al. 1998). The α2A-AR is coupled to Gi/o subset of heterotrimeric G-proteins, which may function against the activation of group I mGluRs which interact with Gq proteins. It is possible that loss of FMRP and inactivation of α2A –AR may lead to epileptogenesis by allowing excessive activation of a common signaling cascade. On the other hand, it is possible that the 2 mutants display similar phenotype of accelerated kindling by employing 2 parallel cellular cascades.

The formation of new synaptic connections is an important process in epileptogenesis. MFS is a major hallmark of abnormal synapse formation that occurs in the epileptic brain (Margerison and Corsellis 1966; McNamara 1999). As FMRP has been shown to effect neuronal elaboration by affecting the function of cytoskeletal proteins (Comery et al. 1997; Irwin et al. 2000; Galvez et al. 2003; Pan et al. 2004; Antar et al. 2006), we investigated MFS in naive and kindled *Fmr1* KO mice. Whereas, the naive *Fmr1* KO brain exhibited no obvious abnormalities in mossy fiber innervation, MFS was dramatically enhanced in the IML region of *Fmr1* KO mice compared with WT mice 5 or 28 weeks after 22 daily stimulations (Fig. 7). This difference was not likely to be simply the result of enhanced seizure activity in the *Fmr1* KO brain because WT mice could be stimulated an additional 8 times (thus 36% more stimulations than *Fmr1* KO mice) and still show little evidence of increased MFS (data not show). Because no obvious neuronal cell death was detected in either the kindled WT or *Fmr1* KO mice 24 h after the completion of kindling development, this enhanced axon reorganization indicates that FMRP may exert an important role in preventing activity-induced neuronal network reorganization in the adult brain.

It has long been known that the cellular and molecular changes that underlie kindling are opposed by refractory periods, but the nature of these changes are not clear (Mucha and Pinel 1977). The upregulation of FMRP expression by kindling-induced seizure as well as the accelerated development of kindling and pervasive seizure-evoked synaptogenesis in *Fmr1* KO mice that we observed together support the idea that FMRP is an important intrinsic buffer against epileptogenesis. It is in this light that we predict that the enhanced susceptibility of patients with FXS to epilepsy is the direct consequence of the absence of a critical homeostatic factor that mitigates vulnerability to excessive neuronal excitation.

Funding

National Basic Research Program of China (2006CB806600); the Key State Research Program of China (2006CB943900); the National "863" high-tech research and development program (2006AA02Z166); the Innovative Research Group of The National Natural Science Foundation of China (30721004); the Chinese Academy of Sciences (KSCX2-YW-R-099). Funding to pay the Open Access publication charges for this article were provided by the Ministry of Science and Technology of the People's Republic of China (the National "863" High-tech Research and Development Program of China 2006AA02Z166).

Notes

Conflict of Interest: None Declared.

Address correspondence to Dr Zhi-Qi Xiong, Institute of Neuroscience, Chinese Academy of Sciences, 320 Yue Yang Road, Shanghai 200031, China. Email: xiongzhiqi@ion.ac.cn.

References

Antar LN, Afroz R, Dictenberg JB, Carroll RC, Bassell GJ. 2004. Metabotropic glutamate receptor activation regulates fragile x mental retardation protein and FMR1 mRNA localization differentially in dendrites and at synapses. J Neurosci. 24:2648–2655.

Antar LN, Li C, Zhang H, Carroll RC, Bassell GJ. 2006. Local functions for FMRP in axon growth cone motility and activity-dependent regulation of filopodia and spine synapses. Mol Cell Neurosci. 32:37–48.

Ashley CT Jr, Wilkinson KD, Reines D, Warren ST. 1993. FMR1 protein: conserved RNP family domains and selective RNA binding. Science. 262:563–566.

Bear MF, Huber KM, Warren ST. 2004. The mGluR theory of fragile X mental retardation. Trends Neurosci. 27:370–377.

Berry-Kravis E. 2002. Epilepsy in fragile X syndrome. Dev Med Child Neurol. 44:724–728.

Brown V, Jin P, Ceman S, Darnell JC, O'Donnell WT, Tenenbaum SA, Jin X, Feng Y, Wilkinson KD, Keene JD, et al. 2001. Microarray identification of FMRP-associated brain mRNAs and altered mRNA translational profiles in fragile X syndrome. Cell. 107:477–487.

Brown V, Small K, Lakkis L, Feng Y, Gunter C, Wilkinson KD, Warren ST. 1998. Purified recombinant FMRP exhibits selective RNA binding as an intrinsic property of the fragile X mental retardation protein. J Biol Chem. 273:15521–15527.

Chen L, Toth M. 2001. Fragile X mice develop sensory hyperreactivity to auditory stimuli. Neuroscience. 103:1043–1050.

Chuang SC, Zhao W, Bauchwitz R, Yan Q, Bianchi R, Wong RK. 2005. Prolonged epileptiform discharges induced by altered group I metabotropic glutamate receptor-mediated synaptic responses in hippocampal slices of a fragile X mouse model. J Neurosci. 25:8048–8055.

Comery TA, Harris JB, Willems PJ, Oostra BA, Irwin SA, Weiler IJ, Greenough WT. 1997. Abnormal dendritic spines in fragile X knockout mice: maturation and pruning deficits. Proc Natl Acad Sci USA. 94:5401–5404.

Croucher MJ, Cotterell KL, Bradford HF. 1995. Amygdaloid kindling by repeated focal N-methyl-D-aspartate administration: comparison with electrical kindling. Eur J Pharmacol. 286:265–271.

Darnell JC, Jensen KB, Jin P, Brown V, Warren ST, Darnell RB. 2001. Fragile X mental retardation protein targets G quartet mRNAs important for neuronal function. Cell. 107:489–499.

Davidovic L, Jaglin XH, Lepagnol-Bestel AM, Tremblay S, Simonneau M, Bardoni B, Khandjian EW. 2007. The fragile X mental retardation protein is a molecular adaptor between the neurospecific KIF3C kinesin and dendritic RNA granules. Hum Mol Genet. 16:3047–3058.

Eberhart DE, Malter HE, Feng Y, Warren ST. 1996. The fragile X mental retardation protein is a ribonucleoprotein containing both nuclear localization and nuclear export signals. Hum Mol Genet. 5:1083–1091.

Gabel LA, Won S, Kawai H, McKinney M, Tartakoff AM, Fallon JR. 2004. Visual experience regulates transient expression and dendritic localization of fragile X mental retardation protein. J Neurosci. 24:10579–10583.

Galvez R, Gopal AR, Greenough WT. 2003. Somatosensory cortical barrel dendritic abnormalities in a mouse model of the fragile X mental retardation syndrome. Brain Res. 971:83–89.

Goddard GV, McIntyre DC, Leech CK. 1969. A permanent change in brain function resulting from daily electrical stimulation. Exp Neurol. 25:295–330.

Greenough WT, Klintsova AY, Irwin SA, Galvez R, Bates KE, Weiler IJ. 2001. Synaptic regulation of protein synthesis and the fragile X protein. Proc Natl Acad Sci USA. 98:7101–7106.

Hagerman RJ, Miller LJ, Grath-Clarke J, Riley K, Goldson E, Harris SW, Simon J, Church K, Bonnell J, Ognibene TC, et al. 2002. Influence of stimulants on electrodermal studies in fragile X syndrome. Microsc Res Tech. 57:168–173.

Hou L, Antion MD, Hu D, Spencer CM, Paylor R, Klann E. 2006. Dynamic translational and proteasomal regulation of fragile X mental retardation protein controls mGluR-dependent long-term depression. Neuron. 51:441–454.

Irwin SA, Christmon CA, Grossman AW, Galvez R, Kim SH, DeGrush BJ, Weiler IJ, Greenough WT. 2005. Fragile X mental retardation protein levels increase following complex environment exposure in rat brain regions undergoing active synaptogenesis. Neurobiol Learn Mem. 83:180–187.

Irwin SA, Galvez R, Greenough WT. 2000. Dendritic spine structural anomalies in fragile-X mental retardation syndrome. Cereb Cortex. 10:1038–1044.

Janumpalli S, Butler LS, MacMillan LB, Limbird LE, McNamara JO. 1998. A point mutation (D79N) of the alpha 2A adrenergic receptor abolishes the antiepileptogenic action of endogenous norepinephrine. J Neurosci. 18:2004–2008.

Jin P, Warren ST. 2003. New insights into fragile X syndrome: from molecules to neurobehaviors. Trends Biochem Sci. 28:152–158.

Li Z, Zhang Y, Ku L, Wilkinson KD, Warren ST, Feng Y. 2001. The fragile X mental retardation protein inhibits translation via interacting with mRNA. Nucleic Acids Res. 29:2276–2283.

Ling SC, Fahrner PS, Greenough WT, Gelfand VI. 2004. Transport of Drosophila fragile X mental retardation protein-containing ribonucleoprotein granules by kinesin-1 and cytoplasmic dynein. Proc Natl Acad Sci USA. 101:17428–17433.

Löscher W, Hönack D. 1991. Anticonvulsant and behavioral effects of two novel competitive N-methyl-D-aspartic acid receptor antagonists, CGP 37849 and CGP 39551, in the kindling model of epilepsy. Comparison with MK-801 and carbamazepine. J Pharmacol Exp Ther. 256:432–440.

Margerison JH, Corsellis JA. 1966. Epilepsy and the temporal lobes. A clinical, electroencephalographic, and neuropathological study of the brain in epilepsy, with particular reference to the temporal lobes. Brain. 89:499–530.

McBride SM, Choi CH, Wang Y, Liebelt D, Braunstein E, Ferreiro D, Sehgal A, Siwicki KK, Dockendorff TC, Nguyen HT, et al. 2005. Pharmacological rescue of synaptic plasticity, courtship behavior, and mushroom body defects in a Drosophila model of fragile X syndrome. Neuron. 45:753–764.

McNamara JO. 1999. Emerging insights into the genesis of epilepsy. Nature. 399:A15–A22.

McNamara JO, Russell RD, Rigsbee L, Bonhaus DW. 1988. Anticonvulsant and antiepileptogenic actions of MK-801 in the kindling and electroshock models. Neuropharmacology. 27:563–568.

Miyashiro KY, Beckel-Mitchener A, Purk TP, Becker KG, Barret T, Liu L, Carbonetto S, Weiler IJ, Greenough WT, Eberwine J. 2003. RNA cargoes associating with FMRP reveal deficits in cellular functioning in Fmr1 null mice. Neuron. 37:417–431.

Mucha RF, Pinel PJ. 1977. Postseizure inhibition of kindled seizures. Exp Neurol. 54:266–282.

Musumeci SA, Bosco P, Calabrese G, Bakker C, De Sarro GB, Elia M, Ferri R, Oostra BA. 2000. Audiogenic seizures susceptibility in transgenic mice with fragile X syndrome. Epilepsia. 41:19–23.

Musumeci SA, Hagerman RJ, Ferri R, Bosco P, Dalla Bernardina B, Tassinari CA, De Sarro GB, Elia M. 1999. Epilepsy and EEG findings in males with fragile X syndrome. Epilepsia. 40:1092–1099.

Nagaraja RY, Grecksch G, Reymann KG, Schroeder H, Becker A. 2004. Group I metabotropic glutamate receptors interfere in different ways with pentylenetetrazole seizures, kindling, and kindling-related learning deficits. Naunyn Schmiedebergs Arch Pharmacol. 370:26–34.

Nosyreva ED, Huber KM. 2006. Metabotropic receptor-dependent long-term depression persists in the absence of protein synthesis in the mouse model of fragile X syndrome. J Neurophysiol. 95:3291–3295.

O'Donnell WT, Warren ST. 2002. A decade of molecular studies of fragile X syndrome. Annu Rev Neurosci. 25:315–338.

Ohashi S, Koike K, Omori A, Ichinose S, Ohara S, Kobayashi S, Sato TA, Anzai K. 2002. Identification of mRNA/protein (mRNP) complexes containing Puralpha, mStaufen, fragile X protein, and myosin Va and their association with rough endoplasmic reticulum equipped with a kinesin motor. J Biol Chem. 277:37804–37810.

Opitz JM, Sutherland GR. 1984. Conference report: international workshop on the fragile X and X-linked mental retardation. Am J Med Genet. 17(1):5–94.

Pan L, Broadie KS. 2007. Drosophila fragile X mental retardation protein and metabotropic glutamate receptor A convergently regulate the synaptic ratio of ionotropic glutamate receptor subclasses. J Neurosci. 27:12378–12389.

Pan L, Woodruff E, III, Liang P, Broadie K. 2008. Mechanistic relationships between Drosophila fragile X mental retardation protein and metabotropic glutamate receptor A signaling. Mol Cell Neurosci. 37(4):747–760.

Pan L, Zhang YQ, Woodruff E, Broadie K. 2004. The Drosophila fragile X gene negatively regulates neuronal elaboration and synaptic differentiation. Curr Biol. 14:1863–1870.

Racine RJ. 1972. Modification of seizure activity by electrical stimulation. II. Motor seizure. Electroencephalogr Clin Neurophysiol. 32:281–294.

Ronesi JA, Huber KM. 2008. Metabotropic glutamate receptors and fragile x mental retardation protein: partners in translational regulation at the synapse. Sci Signal. 1:e6.

Sabaratnam M, Vroegop PG, Gangadharan SK. 2001. Epilepsy and EEG findings in 18 males with fragile X syndrome. Seizure. 10:60–63.

Sato K, Morimoto K, Okamoto M. 1988. Anticonvulsant action of a non-competitive antagonist of NMDA receptors (MK-801) in the kindling model of epilepsy. Brain Res. 463:12–20.

Sobesky WE, Taylor AK, Pennington BF, Bennetto L, Porter D, Riddle J, Hagerman RJ. 1996. Molecular/clinical correlations in females with fragile X. Am J Med Genet. 64:340–345.

Sutula T, Cascino G, Cavazos J, Parada I, Ramirez L. 1989. Mossy fiber synaptic reorganization in the epileptic human temporal lobe. Ann Neurol. 26:321–330.

The Dutch–Belgian Fragile X Consortium. 1994. Fmr1 knockout mice: a model to study *fragile X* mental retardation. Cell. 78:23–33.

Todd PK, Mack KJ. 2000. Sensory stimulation increases cortical expression of the fragile X mental retardation protein in vivo. Brain Res Mol Brain Res. 80:17–25.

Todd PK, Malter JS, Mack KJ. 2003. Whisker stimulation-dependent translation of FMRP in the barrel cortex requires activation of type I metabotropic glutamate receptors. Brain Res Mol Brain Res. 110:267–278.

Turner G, Daniel A, Frost M. 1980. X-linked mental retardation, macro-orchidism, and the Xq27 fragile site. J Pediatr. 96:837–841.

Verkerk AJ, Pieretti M, Sutcliffe JS, Fu YH, Kuhl DP, Pizzuti A, Reiner O, Richards S, Victoria MF, Zhang FP. 1991. Identification of a gene (FMR-1) containing a CGG repeat coincident with a breakpoint cluster region exhibiting length variation in fragile X syndrome. Cell. 65:905–914.

Warren ST, Nelson DL. 1994. Advances in molecular analysis of fragile X syndrome. JAMA. 271:536–542.

Watanabe Y, Johnson RS, Butler LS, Binder DK, Spiegelman BM, Papaioannou VE, McNamara JO. 1996. Null mutation of c-fos impairs structural and functional plasticities in the kindling model of epilepsy. J Neurosci. 16:3827–3836.

Weiler IJ, Irwin SA, Klintsova AY, Spencer CM, Brazelton AD, Miyashiro K, Comery TA, Patel B, Eberwine J, Greenough WT. 1997. Fragile X mental retardation protein is translated near synapses in response to neurotransmitter activation. Proc Natl Acad Sci USA. 94:5395–5400.

Wong RK, Bianchi R, Taylor GW, Merlin LR. 1999. Role of metabotropic glutamate receptors in epilepsy. Adv Neurol. 79:685–698.

Yan QJ, Rammal M, Tranfaglia M, Bauchwitz RP. 2005. Suppression of two major Fragile X Syndrome mouse model phenotypes by the mGluR5 antagonist MPEP. Neuropharmacology. 49:1053–1066.

Zalfa F, Giorgi M, Primerano B, Moro A, Di PA, Reis S, Oostra B, Bagni C. 2003. The fragile X syndrome protein FMRP associates with BC1 RNA and regulates the translation of specific mRNAs at synapses. Cell. 112:317–327.

Zhang YQ, Bailey AM, Matthies HJ, Renden RB, Smith MA, Speese SD, Rubin GM, Broadie K. 2001. Drosophila fragile X-related gene regulates the MAP1B homolog Futsch to control synaptic structure and function. Cell. 107:591–603.